Multi-hop Transmission in Millimeter Wave WPAN with Directional Antenna

by

Jian Qiao

A thesis
presented to the University of Waterloo
in fulfillment of the
thesis requirement for the degree of
Master of Applied Science
in
Electrical and Computer Engineering

Waterloo, Ontario, Canada, 2010

I hereby declare that I am the sole author of this thesis. This is a true copy of the thesis, including any required final revisions, as accepted by my examiners.

I understand that my thesis may be made electronically available to the public.

Abstract

Millimeter-wave (mmWave) communications is a promising enabling technology for high rate (Giga-bit) multimedia applications. However, because oxygen absorption peaks at 60 GHz, mmWave signal power degrades significantly over long distances. Therefore, a traffic flow transmitting over multiple short hops is preferred to improve the flow throughput. In this thesis, we first design a hop selection metric for the piconet controller (PNC) to select appropriate relay hops for a traffic flow, aiming to improve the flow throughput and balance the traffic loads across the network. We then propose a multi-hop concurrent transmission (MHCT) scheme to exploit the spatial diversity of the mmWave WPAN by allowing multiple communication links to transmit simultaneously. By deriving the probability that two links can transmit simultaneously as a function of link length, the MHCT scheme is capable of improving spatial multiplexing gain in comparison with the single hop concurrent transmission (SHCT) scheme. We theoretically demonstrate that by properly breaking a single long hop into multiple short hops, the time resource can be utilized more efficiently, thus supporting more traffic flows in the network within the same time interval. In addition, the per-flow throughput is obtained analytically. Extensive simulations are conducted to validate the analysis and demonstrate that the proposed MHCT scheme can significantly improve the average traffic flow throughput.

Acknowledgements

Since starting at the University of Waterloo, many of my lifelong lessons were taught by individuals who are probably unaware of their impressions on me over the years.

I express the deepest appreciation and gratitude to Professor Sherman (Xuemin) Shen, who has provided his exceptional insight and consultation in the development of my research interests. He has positively influenced me in many ways. His novel ideas, infectious enthusiasm and intellectually stimulating discussions kept me motivated and encouraged through the entire course of my Graduate Studies.

I would like to acknowledge Dr. Lin X. Cai, who has been invaluable as a research partner and friend. This thesis is based upon our joint research, and only with her dedication, wisdom, and inspiration, could I have completed everything on time.

Thank you Professor Jon W. Mark and Professor Liang-Liang Xie for reading my thesis and attending my seminar milestone and of course, for your insights.

I would like to thank Ms. Xiaoxia Zhang, Susan Bian, Sanying Li, Mr. Hao Liang, Hangguan Shang, Tom Luan, Yongkang Liu, Wei Cai, Yanfei Fan, Xiaohui Liang, Khaled Ali, Nizar H. Alsharif, who give me support for discussions and co-operation.

Thank you everyone for your belief in me.

Dedication

For the most loving Father and Mother, who sacrificed all for our destinies.

Contents

List of Tables viii

List of Figures x

1 Introduction 1

1.1 Millimeter Wave WPAN 2

1.2 Motivation and Research Issues 6

1.3 Organization of Thesis 8

2 Background 9

2.1 Related Works 10

2.2 Thesis Contributions 12

3 System Model 14

3.1 mmWave Communication 14

3.2 Antenna Model 16

3.3 Directional MAC Structure 16

4 Multi-hop Concurrent Transmission Scheme **19**

4.1 Hop Selection Metric 20

4.2 Proposed Concurrent Transmission Scheme 22

5 Performance Analysis **26**

5.1 Spatial Multiplexing 26

5.2 Time Division Multiplexing 31

5.3 Per-Flow Throughput 36

6 Performance Evaluation **39**

6.1 Average Flow Throughput 41

6.2 Network Throughput 42

7 Conclusions **44**

7.1 Future works 45

References **53**

List of Tables

6.1 SIMULATION PARAMETERS 40

List of Figures

1.1 Millimeter Wave Bands in Various Countries 2

1.2 Free Space Path loss at 60 GHz 4

1.3 Wireless Personal Area Network Architecture 5

1.4 Achievable Flow Throughput with Various Number of Hops 7

2.1 The Classification of Wireless MAC Protocols. 11

3.1 The Radiation Pattern of Directional Antenna. 17

3.2 IEEE 802.15.3 MAC Structure 17

4.1 Illustration for Hop Selection 22

5.1 Concurrent Transmissions in WPAN 27

5.2 Probability P versus Link Length 30

5.3 Illustration for Time Division Multiplexing 32

5.4 Probability Distribution Function of Link Length 35

5.5 Time Division Multiplexing 37

6.1 Node Placement for Simulation Scenario 41

6.2 Average Flow Throughput versus Various Number of Traffic Flows 42

6.3 Network Throughput versus Various Number of Traffic Flows 43

Chapter 1

Introduction

Communications at 60 GHz band is referred to as millimeter-wave (mmWave) communications because the wavelength at this band is in the order of millimeters. Within the past decade, the wireless communication community has become increasingly interested in worldwide 60 GHz radio frequency band [1–8]. It has been considered as one of the most promising candidates for both indoor and outdoor wireless communications within a short range and has been attracting more and more efforts in research, development, regulation, and standardization. In 2001, the Federal Communications Commission (FCC) has approved an un-precedented 7 GHz spectrum between 57 and 64 GHz for general use. Japan has released the 59−66 GHz band for unlicensed usage. In Europe, there is a consideration by the European Conference of Postal and Telecommunications Administrations (ECPT) to allocate 54−66 GHz for the same purpose. Other governments also have similarly allowed portions of the 60 GHz band to be used without a license (see Fig. 1.1). The large bandwidth enables multi-Gbps wireless connections for high data rate-demand communications. Several standardization groups, such as IEEE 802.15.3c [9], IEEE 802.11 VHT [10] and ECMA international TC48 [11], are ongoing to develop a standard mmWave system to realize this multi-Gbps transmission. Key to the creation of millimeter-wave WPAN

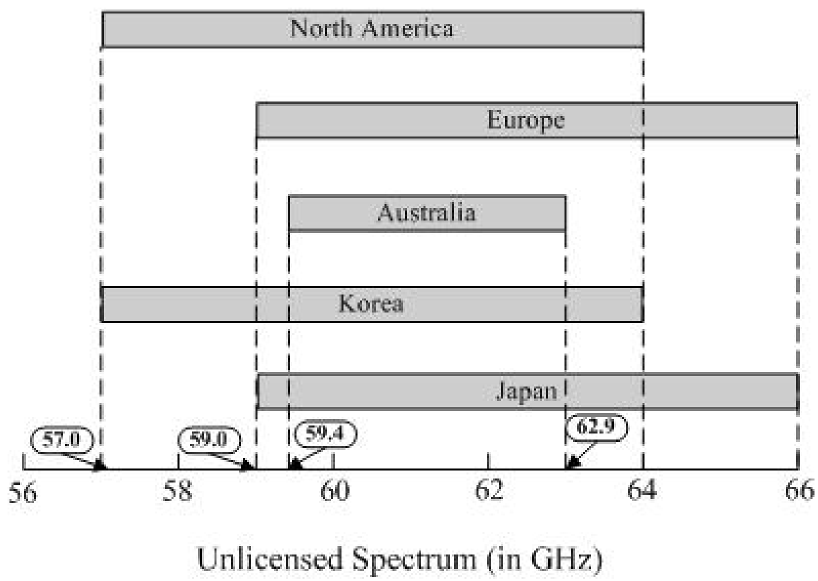

Figure 1.1: Millimeter Wave Bands in Various Countries

is the development of cost-effective technologies that support very high throughput. In the thesis, a multi-hop concurrent transmission scheme is proposed to improve the flow throughput and network throughput by fully exploring the spatial reuse and time division multiplexing gain. The network throughput is defined as the total traffic throughput of all the traffic flows in the network.

1.1 Millimeter Wave WPAN

The new applications for wireless personal area network (WPAN) require very high data rates with isochronous data delivery. Because of the high expectations of the user, a very high level of QoS will be required to satisfy their desires. The millimeter-wave (mmWave) frequencies, particularly the 60 GHz unlicensed spectrum, provide a unique opportunity to wirelessly enable these applications. In particular, the 60 GHz unlicensed band provides the following advantages:

- Huge frequency allocation. Typically 7 GHz in most regions, with 5 GHz of overlapping allocations.

- Much more power available. Unlike the strict transmit power restrictions on UWB unlicensed operation, the mmWave band allows an effective isotropic radiated power that is significantly greater.

- Clean spectrum, no incumbents. There are not any widely deployed 60 GHz radiators in the home or office, so there is less chance for interference.

- High frequency allows small, high-gain antennas. A 25-dB gain antenna has an effective aperture approximately one square inch. High-gain antennas allow high EIRP with low-power RF amplifiers

- High gain allows overlapping networks that don't interfere each other. Because the antennas are highly directional at these frequencies, spatial reuse is enabled.

mmWave bands have their own characteristics different from lower frequency bands, which are considered in our proposed multi-hop concurrent transmission scheme. One fundamental distinguishing feature of mmWave communications is the high propagation loss as shown in Fig. 1.2. As the free space propagation loss increases proportionally with the square of the carrier frequency, the propagation loss at mmWave band is much higher compared with other lower frequency bands, e.g., 28 dB higher than at 2.4 GHz. The path loss becomes more serious since oxygen absorption peaks at 60 GHz. Directional antenna with high directivity gain is utilized to combat the severe path loss and achieve high data rate in mmWave channels. On the other hand, the high path loss and the utilization of directional antenna allow more efficient space reuse. Signals at lower frequency bands can easily traverse through building materials, however mmWave signals cannot penetrate solid materials very well. Consequently, mmWaves permit a dense packing of communication frequencies, thus providing very efficient spectrum utilization, and increasing the

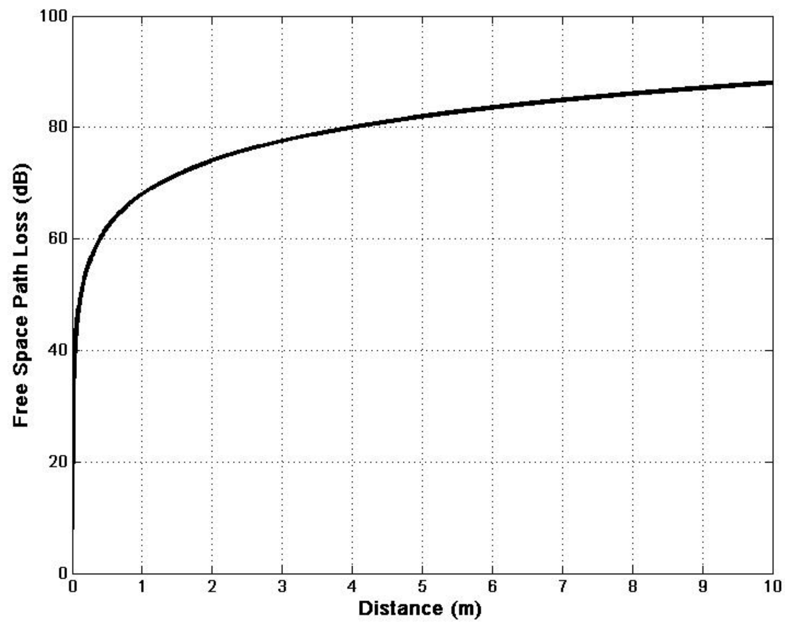

Figure 1.2: Free Space Path loss at 60 GHz

security of transmissions. Moreover, like light waves, millimeter-wave signals result in low diffraction, but are subject to more shadowing and reflection. For non-line-of-sight (NLOS) propagation, the greatest contribution at the receiver is the reflected power. Shorter wavelengths cause the reflecting material to appear relatively rougher, which results in greater diffusion of the signal and less direct reflection. Since diffusion provides less power at the receiver than directly reflected power, millimeter-wave systems usually rely on line-of-sight (LOS) communication link. Directional antennas are normally required in these systems to achieve reliable communication and spatial reuse.

Apart from this, mmWave systems share common features with other wireless systems. These include: (1) high error rate and bursty errors; (2) location-dependent and time-varying wireless link capacity; (3) half-duplex communication; (4) user mobility; and (5) power constraints of mobile users.

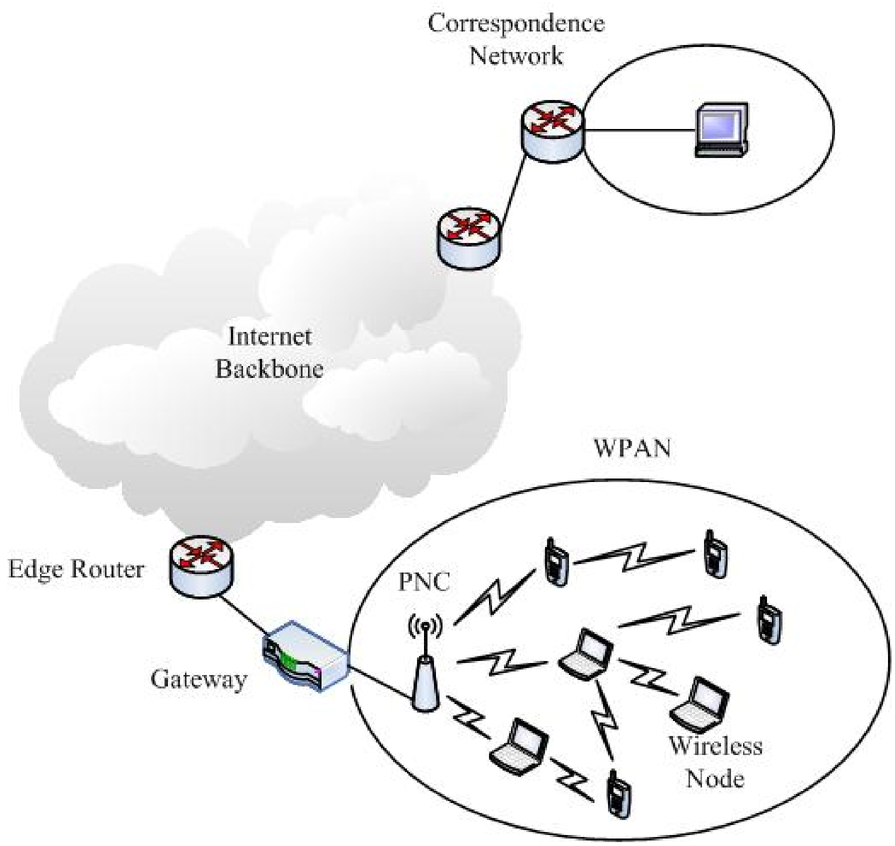

Figure 1.3: Wireless Personal Area Network Architecture

On one hand, our proposed multi-hop concurrent transmission scheme should match the application scenario of mmWave WPAN and satisfy general design rules such as efficiency and scalability. On the other hand, it should take into account the unique characteristics exhibited in millimeter-wave bands.

The mmWave WPAN are designed to provide multi-Gbps data rate to enable applications including audio, digital video, HDTV, media-rich interactive games, and data applications running on portable devices, laptops, home theater, and other consumer electronics. The IEEE 802.15.3c standard defines five usage models based on various market use-cases: uncompressed video streaming (P2P), multi uncompressed video streaming (P2MP), office desktop, conference ad-hoc, and Kiosk file-downloading. The usage models specify one or more applications and environments from which a simulation scenario can be created once the traffic patterns of the applications are known. As shown in Fig. 1.3, the basic topology unit of WPAN is piconet, which is formed in an ad hoc manner and composed of several wireless nodes (WNs) and a single piconet controller (PNC). As its name suggested, the piconet is confined to a small area, typically covering a range of about 10 meters. This is the range a millimeter-wave system usually covers in an indoor environment. In order to share frequency resources among different piconets, neighbor piconets are used to provide coexistence due to the large path loss at mmWave band.

1.2 Motivation and Research Issues

The unique features of mmWave communications, i.e., high path loss, spatial reuse and LOS connection, benefit and motivate us to use multi-hop concurrent transmission. As mmWave signals attenuate significantly over distance, a traffic flow transmitting over multiple short hops can achieve much higher flow throughput than that over a single long hop in a mmWave channel. Fig. 1.4 shows the achievable data rate for multi-hop traffic flows without consideration of intra-flow concurrent transmissions. The hops for each traffic flow are of the same length. For longer transmission distance, it is shown that multi-hop transmission can achieve higher flow throughput than that of single hop transmission even if there are no intra-flow concurrent transmissions. To leverage the transmission data rate over distance, appropriate multi-hop relaying plays a critical role. This thesis studies how to select relay nodes to improve the flow throughput and network throughput. In specific, a novel hop selection metric is designed for the piconet controller (PNC) to choose proper relay nodes to forward data, aiming to improve the flow throughput and distribute the traffic load across the network. To further improve the network performance, we propose a multi-hop concurrent transmission (MHCT) scheme to allow non-interfering

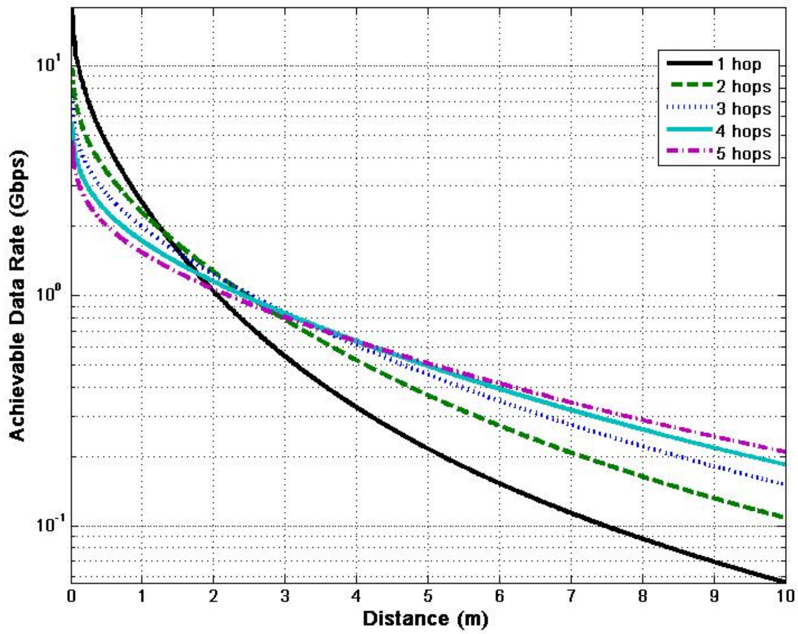

Figure 1.4: Achievable Flow Throughput with Various Number of Hops

communication links to concurrently transmit over a mmWave channel by exploring the spatial reuse. By properly breaking one long-hop (i.e., low rate) transmission into multiple short-hop (i.e., high rate) transmissions and allowing some non-interfering hops to transmit concurrently, the network capacity can be efficiently improved in terms of flow throughput and network throughput. In addition, as indicated in [12], the multi-hop transmission scheme can overcome the problem of link outage due to obstacles and moving people in indoor mmWave WPAN.

1.3 Organization of Thesis

The thesis is organized as follows. Chapter 2 provides a background on transmission schemes in mmWave WPAN. In Chapter 3, the system model that our scheme is based on, is described. A multi-hop concurrent transmission scheme with a hop selection metric is proposed in Chapter 4, to select proper relays for each traffic flow and allow non-interfering communication links to transmit concurrently. Spatial and time division multiplexing gains are analyzed in Chapter 5. Chapter 6 presents performance evaluation and numerical results. Chapter 7 provides the concluding remarks, which summarize the contributions of this research and state the future works to be addressed on mmWave WPAN systems.

Chapter 2

Background

There is increasing interest in pushing wireless data rates beyond Gbps in order to more rapidly access data on personal devices, as well as potentially replace all the cables going into a device, including the video cable. One means of achieving this is through the use of mmWave WPAN which take advantages of short separation distances, wide bandwidths on the order of several GHz, and advanced signal process techniques including MIMO, advanced FEC, and higher-order modulation techniques. However, further research is needed for achieving Gbps rates in low-cost and low-power devices, ranging from low power RF and high-speed digital circuits [13–15] to MAC layer protocols [16–21] to overall systems design [12, 22]. The interest of the thesis is in the transmission scheme for MAC protocol for mmWave WPAN.

Wireless MAC protocols can be broadly classified into two categories: distributed and centralized protocols. In distributed protocols, competing nodes in the network contend for medium access without any centralized coordination. On the other hand, in centralized protocols, there is a special node responsible for channel allocation. Based on the method of operation, the MAC protocols are further divided into three access modes: random access, guaranteed access, and hybrid access (see Fig. 2.1). The thesis uses a centralized and hybrid access mode for MAC protocol. Hybrid access protocols are based on request-grant mechanisms; i.e., each node sends a request to the coordinator indicating the bandwidth it requires, using random access. If a request is successful, it joints the request queue and time slots are allocated at latter time.

Optimizing resource utilization for wireless networks has been an active research topic because wireless resource is at a premium. Since wireless communication is broadcast in nature, flow throughput and network throughput are limited by interference and collisions. It is essential to utilize the resource efficiently in mmWave WPAN to achieve high network throughput and flow throughput, while allowing more users in the network. Traditionally, the transmission in WPAN is usually one-hop due to the limited network range, on order of 10 meters. However, for mmWave WPAN, due to the characteristics described in Chapter 1, multi-hop transmission has several advantages. TDMA transmission mode is that only one transmission is allowed in the network at any time. In other word, TDMA system without time-slot reuse mechanism conventionally allocates one TDMA time-slot to only one communication link at a time. It can avoid interference and collisions, but does not utilize the network resource efficiently. Concurrent transmission, taking the advantages of large path loss in mmWave band and the utilization of directional antenna, can allow multiple communication links to transmit concurrently, thus significantly increases network throughput.

2.1 Related Works

Recognizing the unique features of mmWave communications, work on directional medium access control (MAC) in mmWave wireless personal area networks (WPAN) has appeared in the literature [12, 23–26]. An architecture is proposed for mmWave WPAN in [12], where an intermediate node is selected as the relay when the LOS link between source

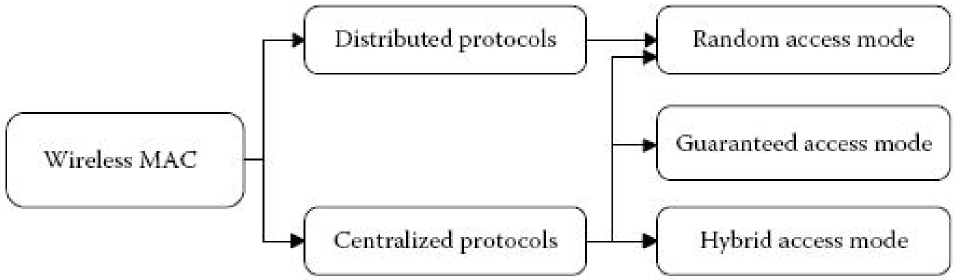

Figure 2.1: The Classification of Wireless MAC Protocols.

and destination is blocked by moving obstacles. The proposed architecture is shown to be effective to keep the network connectivity when serious link outage happens due to moving obstacles. In [23], an exclusive region (ER) based resource management scheme is proposed to explore the spatial multiplexing gain of mmWave WPAN with directional antenna and the optimal ER sizes are analytically derived in [24]. To improve the network capacity, multiple traffic flows that do not cause harmful interference to each other are scheduled for concurrent transmissions.

Although one of the challenges of 60 GHz systems is the severe attenuation experienced when operating at such high frequencies, this can be turned into an advantage when trying to reuse the spectrum in a small area. In [26], a method for coordinating time-slot allocations is proposed, based on measured interference in order to allow non-interfering devices to occupy the same time-slots in an area in order to enhance the aggregate throughput of the system.

A MAC layer beamforming protocol following the guidelines of the IEEE 802.15.3c criteria for mmWave 60-GHz WPAN is proposed in [27]. The authors consider simple beam codebooks such that each element in a phased antenna array only has four phase shifts (0, 90, 180, 270) and no amplitude adjustment. The authors show that a large reduction of beamforming setup time is possible using their proposed technique as opposed to brute force searching.

Since it is envisioned that 60 GHz WPAN systems will be carrying many different kinds of data and multi-media traffic, it is important to support different kinds of access methods, namely TDMA for high quality-of-service links, as well as CSMA/CA for rapid access to the channel for data or control information. The current IEEE 802.15.3c standard which includes a hybrid MAC capability is studied in [28], and it also evaluates a method for optimizing the throughput of the system by reducing the collisions in the CSMA/CA time-slots using a private channel release time. This feature is shown to help significantly increase the available throughput of the IEEE 802.15.3c network.

In [29], the potential for spatial reuse and the degree of interference is evaluated for 60 GHz indoor wireless communication systems. Simulations are made in indoor environments by varying parameters affecting the spatial reuse and aggregate data rates. The results show that there is high potential of spatial reuse and also there are considerable cases in which interference mitigation mechanisms are needed to improve spatial capacity of 60 GHz systems.

To the best of our knowledge, the previous works in mmWave MAC design use single hop for data transmission or just use one relay if LOS is unavailable.

2.2 Thesis Contributions

The main contributions of the thesis are four-fold. First, a novel metric is designed to select relay hops to forward data for multi-hop flows. Second, we propose a concurrent transmission scheduling algorithm to explore the spatial multiplexing gain in mmWave WPAN, considering the unique features of mmWave communications, e.g., the link outage due to moving obstacles and the utilization of directional antenna. Third, it is demonstrated that the MHCT scheme can utilize the spatial resource more efficiently because of the larger concurrent transmission probability, resulting from the shorter link length compared with SHCT scheme. We also derive the conditions to ensure that MHCT outperforms SHCT on time division multiplexing in terms of required number of time slots. Finally, given a transmission schedule, the per-flow throughput is calculated theoretically. Extensive simulations are also conducted to demonstrate the efficiency of the proposed scheme and verify the accuracy of the analysis.

Chapter 3

System Model

We consider an indoor WPAN composed of several wireless nodes (WNs) and a single piconet controller (PNC). Each node in the network is equipped with an electronically steerable directional antenna. Both transmitters and receivers direct their beams towards each other for data transmission. Due to the severe path loss and utilization of directional antenna, we allow non-conflicting communication links to transmit concurrently in TDM mode. Because of the accurate localization service provided by the Ultra-wideband system, we assume the PNC has the topology information of the network. Moving obstacles greatly degrade the transmission data rate especially if they are located in the LOS path between two nodes. Therefore, the multi-hop concurrent transmission scheme is based on LOS link of each hop.

3.1 mmWave Communication

According to Shannon theory, the achievable data rate in an additive white Gaussian noise (AWGN) channel is:

$$C = W\log_2[1 + \frac{P_R}{(N_0 + I)W}] \tag{3.1}$$

where P_R is the received signal power, W is the system bandwidth, N_0 and I are the one-side power spectral density of white Gaussian noise and interference respectively.

We apply the Friis transmission equation to calculate the received power in a free space, which is a function of transmission range r,

$$P_R(r) = P_T G_R G_T (\frac{\lambda}{4\pi d})^2 \tag{3.2}$$

where P_T is the transmission power, G_T and G_R are the antenna gains of the transmitter and receiver respectively, λ is the wavelength and d is the transmission distance between the transmitter and the receiver. Considering multipath fading and signal dispersion, the received signal power is

$$P_R(r) = P_T G_R G_T (\frac{\lambda}{4\pi})^2 (\frac{1}{d})^n \tag{3.3}$$

where n is the path loss exponent which can be determined experimentally and is usually in the range of 2 to 6 for indoor environment [30]. Combining equation (3.1) and equation (3.3), the data rate is obtained as

$$C = W\log_2[1 + \frac{P_T G_R G_T \lambda^2}{16\pi^2 (N_0 + I) W d^n}] \tag{3.4}$$

In equation (3.4), it can be seen that the minimum hop-count metric which usually favors the hop with long distance, significantly reduces the received signal strength and degrades the achieved traffic flow throughput. According to equation (3.4), the flow throughput deduction over distance is more serious in mmWave system due to its large bandwidth and small wavelength. Thus it is likely to improve the flow throughput by replacing single long hop by multiple short hops.

3.2 Antenna Model

We apply an ideal "flat-top" model for directional antenna [31]. Every node employs an antenna with N beams, each of which spans an angle of $2\pi/N$ radians. Each beam has a fixed beamwidth with none overlapping beam radians so that N beams can collectively maintain the seamless coverage for the entire plane. Directional antennas are characterized by their pattern functions that measure the power gain $G(\phi)$ over the angle ϕ. The normalized pattern function is defined as

$$g(\phi) = \frac{G(\phi)}{G_{max}}, \tag{3.5}$$

where

$$G_{max} = max_{\phi} G(\phi). \tag{3.6}$$

In an ideal case, the antenna gain is constant, i.e., unit gain, within the beamwidth and zero outside,

$$g(\phi) = \begin{cases} 1, & \mid \phi \mid \leq \dfrac{\Delta\phi}{2} \\ 0, & \text{otherwise} \end{cases} \tag{3.7}$$

where $\Delta\phi = 2\pi/N$ is the antenna beanwidth. In our system, both the transmitters and receivers use directional antenna for data transmissions, thus the antenna gains of transmitters and receivers, $G_T = G_R = 1$ within the antenna beamwidth and $G_T = G_R = 0$ outside. Fig. 3.1 shows a radiation pattern with 6 beams based on the "flat-top" model, i.e., the beamwidth is 60 degrees.

3.3 Directional MAC Structure

The MAC protocol is based on IEEE 802.15.3 superframe structure, as shown in Fig. 3.2. A superframe consists of three periods, beacon period, random access period and data

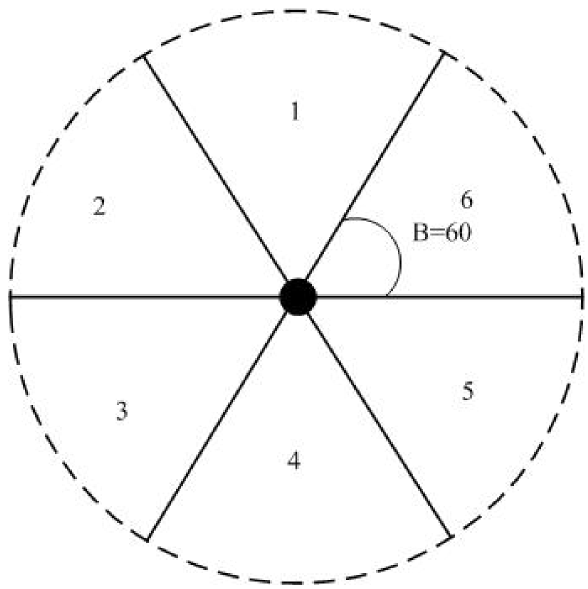

Figure 3.1: The Radiation Pattern of Directional Antenna.

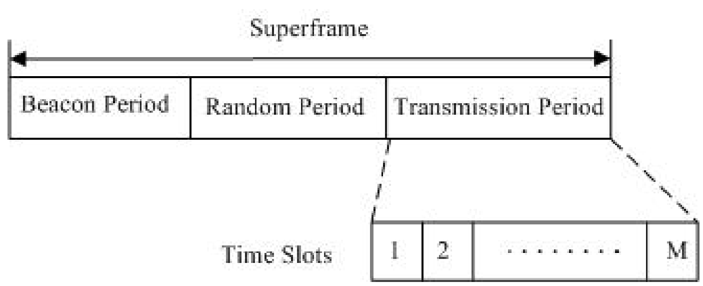

Figure 3.2: IEEE 802.15.3 MAC Structure

transmission period. During the beacon period, the PNC activates all its beams and sends out beacon frames in all directions to other nodes for synchronization, scheduling information and other management information distribution. The scheduling information includes the transmission start time, a maximum allowed transmission (TXOP) duration and antenna beam direction. The beacon period is followed by a random access period during which the nodes send transmission requests, topology information and load information to the PNC, based on which the PNC schedules contention-free peer-to-peer transmissions in the following data transmission period. To avoid deafness problem caused by directional antenna which invokes very complicated MAC design, the PNC still operates in the omni-directional mode by switching all its beams on in the random access period while it can use one beam for data transmission in the following data transmission period. To fully exploit the mmWave channel capacity, we improve the IEEE 802.15.3 MAC by allowing multiple nodes to concurrently transmit. Two transmissions can operate simultaneously if and only if one receiver is outside the beamwidth of the other transmitter, given that the transmitter and receiver always steer beams to each other [23, 32].

Chapter 4

Multi-hop Concurrent Transmission Scheme

Multi-hop transmission means that a flow from a source is capable of reaching the destination over multiple hops. A hop is formed between two nodes by aligning the directional antennae on each other. Unlike wireline networks, there are unique characteristics of mmWave WPAN:

- Due to half-duplex constraint, the nodes in the network can only send or receive at a given time, i.e., the adjacent hops can not transmit data simultaneously.
- In mmWave WPAN with directional antennae, directivity and high path loss allow non-interfering hops to transmit concurrently over mmWave channel.
- Millimeter-wave band path loss is severe with distance and flow throughput improvement can be achieved by replacing single long hop with multiple short hops, even if the intra-flow hops can not transmit concurrently.

In this chapter, a hop selection metric is proposed to determine a multi-hop path for a traffic flow to increase the flow throughput and achieve load-balancing. Based on the metric, then a multi-hop concurrent transmission algorithm is presented to improve the spatial capacity of mmWave WPAN. The basic idea is that PNC collects the global user information to select an appropriate multi-hop path for each traffic flow and allow non-conflict hops to transmit concurrently.

4.1 Hop Selection Metric

To achieve high transmission data rate for each traffic flow, short links are usually preferred in hop selection. Therefore, more hops may be involved in each flow, which results in heavy traffic loads in the network. In addition, when traffic aggregates at some of the nodes, congestion may occur and these nodes become bottleneck for the network. Therefore, we need to select appropriate relay hops to improve the network throughput, considering both the link length and the traffic loads at the nodes.

When the PNC receives a request, it determines appropriate relaying hops based on the global network information, including the distance from one node to all its neighbors, antenna directions steering to their neighbors, and the traffic load of each node. The traffic load of each node is defined as the traffic at each node before the scheduled transmission over this hop starts. More concurrent transmissions can be supported by well balancing the traffic loads among multiple nodes in the network. To determine the relaying hops for a pair of transmitter and receiver, a weighted graph is generated by the PNC based on the topology information and traffic loads of each node. The weight associated with link $(A \rightarrow B)$ between nodes A and B is given as

$$w(A,B) = \frac{d^2(A,B)}{\overline{d^2}} + \frac{F(B)}{\overline{F}} \tag{4.1}$$

where $d(A, B)$ is the link length of link $(A \rightarrow B)$; $F(B)$ is the traffic load of node B. $\overline{d^2}$and $\overline{F}$ are the average link length square and average traffic loads of each node, respectively. We use normalized traffic load and link length square for hop selection to smooth the large difference between the node's loads and link lengths. To achieve load balancing and improve flow throughput, link length square and node's load should equally contribute to the hop selection. We use link length square rather than link length to favor multiple hops with shorter links. In other words, the first item in the metric provides high data rate while the second item reduces the traffic loads aggregation. For example, as shown in Fig. 4.1, there are three options from source to destination, $S \rightarrow A \rightarrow D$, $S \rightarrow A \rightarrow C \rightarrow D$ and $S \rightarrow B \rightarrow C \rightarrow D$. According to above hop selection metric, given link lengths and node loads, the weights of the three options are in the following sequence $W_{S \rightarrow A \rightarrow D} > W_{S \rightarrow A \rightarrow C \rightarrow D} > W_{S \rightarrow B \rightarrow C \rightarrow D}$ while $W_{S \rightarrow A \rightarrow C \rightarrow D} > W_{S \rightarrow B \rightarrow C \rightarrow D} > W_{S \rightarrow A \rightarrow D}$ if the link square item in equation (4.1) is replaced by link length. Our analysis in the section of mmWave communication shows that the option $S \rightarrow B \rightarrow C \rightarrow D$ is more likely to achieve higher flow throughput in comparison with the others and the traffic load has large impact on hop selection if there are more traffic flows in the network. The hops with minimum accumulated weights from the source to the destination are chosen for the traffic flow to transmit data. The hops selected for each traffic flow depend on the network topology, but based on the proposed metric we can obtain insights on hop selection for a dense and load-balanced mmWave WPAN: 1) the selected relay nodes should be close to or on the line between source and destination; 2) the accumulated weights achieve the minimum value if the lengths of selected hops for each flow are almost the same; 3) with more short hops for each traffic flow, the accumulated value of link length square decreases while the accumulated value of node loads increase. This tradeoff bounds the number of hops for each flow.

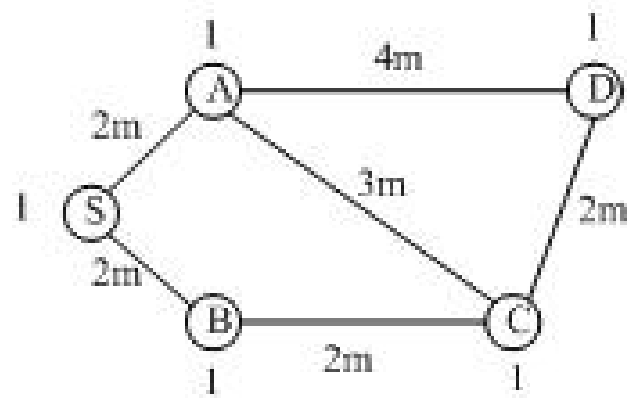

Figure 4.1: Illustration for Hop Selection

4.2 Proposed Concurrent Transmission Scheme

The proposed multi-hop concurrent transmission scheme is based on the hop selection metric designed above. The details on the proposed scheme are given as follows: during the random access period, the PNC activates all the beams to collect global user information, e.g., topology information and traffic loads. When a transmission request is received, the PNC calculates $\overline{d^2}$ and $\overline{F}$ based on the traffic load and topology information received in random access period, and then generates a weighted graph where each link has a weight as equation (4.1). The PNC calculates accumulated weights for each flow by summing up the weights of each hop along the path from source to destination together. The hops with the lowest accumulated weights are chosen. The PNC then checks if these hops can transmit concurrently with the hops which has been scheduled. During the beacon period, the PNC distributes the scheduling information to all the nodes with data ready to transmit. It is possible that a WN (wireless node) sends a transmission request to PNC but does not receive the scheduling information within a certain time interval (e.g., a random access period plus a beacon period) because moving obstacles in the room may block the LOS link. This WN needs to send another transmission request in the next random access period accordingly. During transmission period, PNC switches to directional mode and acts as pseudo WN for data transmission. The nodes begin to transmit data according to the scheduling information. If the data transmission is not successful due to blocked LOS by moving obstacles, the failures should be reported to the PNC during next random access period so that the PNC can re-schedule the transmission in the next transmission period.

Next, we develop the scheduling algorithm for concurrent transmissions during the transmission period. In some case, due to the network topology, some hops in a dense area have lower probability to transmit concurrently with other hops. Therefore, we need to give the hop, which has less transmission opportunity but higher traffic loads, a higher priority to be scheduled. To achieve this, we sort hops in the descending sequence based on the number of transmission loads to guarantee that the hops with highest loads will be scheduled first. The detailed algorithm is described as follows. Initially, there are L slots in a transmission period. A transmission request $r_{i,j}$ (jth hop for ith flow) needs $n(i, j)$ slots. The PNC sequentially checks the hops to be scheduled in the descending order of their traffic loads, thus gives highly loaded link a higher priority for data transmission. The PNC checks the concurrent transmission condition by comparing the radiation angles of all the transceivers in this group.

The PNC also needs to check whether in this group there are adjacent hops which share one common node as a receiver or transmitter. This check is necessary because a wireless node operating in a half-duplex mode can not receive and transmit simultaneously. If the link does not conflict with all existing hops in the group, this link can be added in the group for concurrent transmission. The PNC updates the reserved slots based on the maximum number of required slots in this group. If a hop conflicts with all existing groups, the PNC needs to create a new group for this hop when the number of available slots is sufficient. Otherwise, the PNC rejects the request due to limited network resources. In this case,

Algorithm 1 Concurrent Transmission Scheduling Scheme

```
BEGIN:
1: PNC receives a request r_{i,j} for n(i,j) time slots
2: for all non-empty group(T_b! = Null) do
3:   if r_{i,j}'s beams does not conflict with those of all existing hops in T_b then
4:     if r_{i,j} does not have shared nodes with other hops in T_b then
5:       if r_{i,j} requires extra slots, n(i,j) − n(b) > 0 then
6:         if Available slots L ≥ n(i,j) − n(b) then
7:           Schedule r_{i,j} in group T_b;
8:           Update T_b = T_b ⋃ {r_{i,j}};
9:           Update the available slots L = L − [n(i,j) − n(b)];
10:          Update n(b) = n(i,j);
11:          Update the allocated slots for r_{i,j};
12:          Sort all hops in the decreasing order of allocated slots.
13:          go to END;
14:        else
15:          go to line 26;
16:        end if
17:      else
18:        Schedule r_{i,j} in T_b;
19:        Update T_b = T_b ⋃ {r_{i,j}};
20:        Update the allocated slots for r_{i,j};
21:        Sort all hops in the decreasing order of allocated slots.
22:        Go to END;
23:      end if
24:    end if
25:  end if
26:  Next Group;
27: end for
28: if Available slots N ≥ n(i,j) then
29:   Start a new group T(k) = {r_{i,j}};
30: else
31:   Reject request r_{i,j} and release resources of all hops in r_{i,j};
32: end if
END;
```

the PNC will remove all hops involved in the flow where the rejected hop belongs to. The pseudo code for the concurrent transmission scheduling algorithm is shown in Algorithm 1.

Chapter 5

Performance Analysis

Multi-hop transmissions are designed to overcome the problem of link outage due to severe path loss of mmWave band and improve flow throughput. Concurrent transmissions are more favorable than serial TDMA transmissions in terms of network throughput improvement by exploiting the spatial reuse of wireless channel [23, 26]. In this chapter, we first analyze the performance of the proposed multi-hop concurrent transmission scheme on spatial reuse and conjecture that the proposed scheme can explore more spatial multiplexing gain than SHCT scheme. We then derive the condition that multi-hop concurrent transmission scheme outperforms SHCT scheme on time division multiplexing.

5.1 Spatial Multiplexing

With short link length, the overlap area between the beamwidth of the receiver and the area of WPAN is likely to be smaller in comparison to that with long link length. Then there are probably more links to be transmitted concurrently in the whole area, according to the concurrent transmission condition. Therefore, the spatial resource can be utilized more efficiently by replacing single long hop with multiple short hops. In the following,

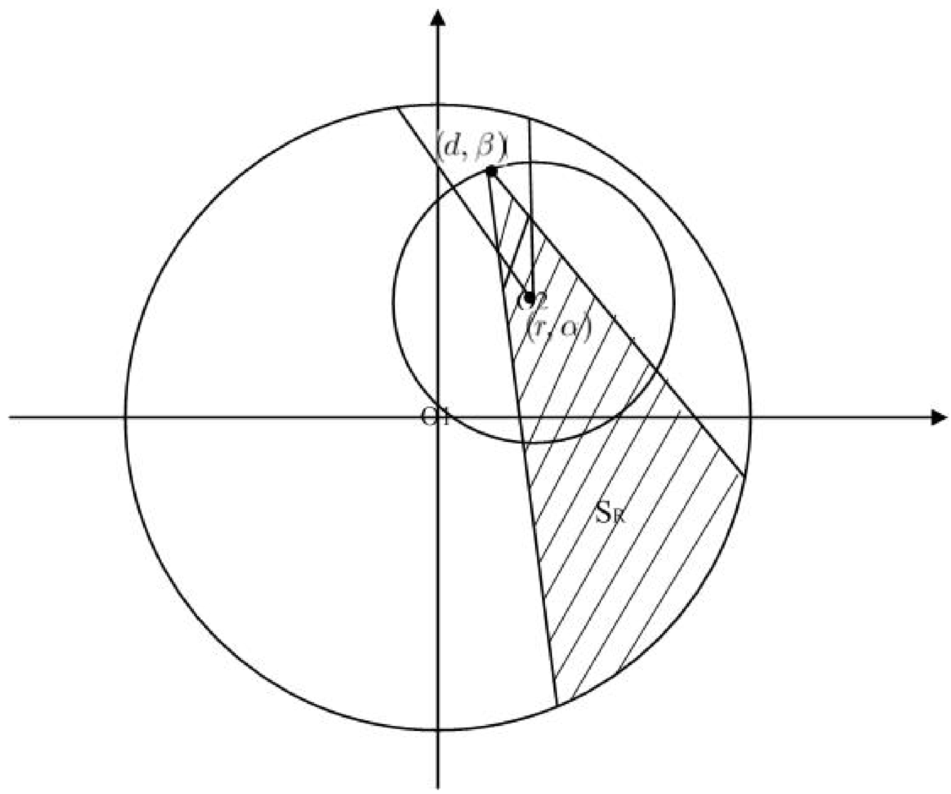

Figure 5.1: Concurrent Transmissions in WPAN

we derive the average concurrent transmission probability as a function of link length and show the spatial multiplexing gain achieved by multi-hop concurrent transmissions.

Consider an indoor WPAN circle area S with radius R. As shown in Fig. 5.1, there are one transmitter and one receiver in the area. The transmitter and receiver are randomly selected and direct their beams to each other for data transmission. S_R is the overlap areas between S and the beamwidth of the receiver. Then the probability that a transmitter lies outside of the beamwidth of the receiver and does not direct its beamwidth to the receiver is

$$P = (1 - \frac{S_R}{S})(1 - \frac{\theta}{2\pi}) \tag{5.1}$$

where θ is the beamwidth of the receiver and the transmitter. The probability that one link does not conflict with another link in the WPAN area is $Q = P^2$. For an extreme case, a long hop with $2R$ as link length is replaced by two hops with R as link length. The probability P can be improved from 0.32 to 0.51 with the beamwidth $\theta = 60°$.

Polar coordinate system O_1 is established with the center of circle area S as the origin. Then the position of transmitter is given by (r, α) in system O_1. Similarly, polar coordinate system O_2 is built with the transmitter as the origin and the position of the corresponding receiver is given by (d, β) in the polar coordinate system O_2. d is the distance between the transmitter and receiver, i.e., link length. Due to symmetry, we only consider the case $0 \leq \alpha \leq \frac{\pi}{2}$. To make the analysis tractable, the overlapping area of S_R is approximated as a triangle.

$$S_R = \begin{cases} \frac{1}{2}g(a,b,\theta)g(a,b,-\theta), & -\frac{\pi}{2}+\frac{\theta}{2} < \beta < \frac{\pi}{2}-\frac{\theta}{2} \\ -\frac{1}{2}g(a,b,\theta)g(-a,-b,-\theta), & \frac{\pi}{2}-\frac{\theta}{2} < \beta < \frac{\pi}{2}+\frac{\theta}{2} \\ \frac{1}{2}g(-a,-b,\theta)g(-a,-b,-\theta), & \frac{\pi}{2}+\frac{\theta}{2} < \beta < \frac{3\pi}{2}-\frac{\theta}{2} \\ -\frac{1}{2}g(-a,-b,\theta)g(a,b,-\theta), & \frac{3\pi}{2}-\frac{\theta}{2} < \beta < \frac{3\pi}{2}+\frac{\theta}{2} \end{cases} \tag{5.2}$$

where $a = r\cos\alpha + d\cos\beta$, $b = r\sin\alpha + d\sin\beta$ and the function $g(a, b, \theta)$ is defined as

$$g(a,b,\theta) = \cos(\beta - \frac{\theta}{2}) \mid \sqrt{\frac{R^2}{\cos^2(\beta-\frac{\theta}{2})} - [a\tan(\beta-\frac{\theta}{2}) - b]^2} + a + b\tan(\beta - \frac{\theta}{2}) \mid \tag{5.3}$$

Substituting (5.2) and (5.3) into (5.1), the probability P is the function of r, α, d and β, $P = P(r, \alpha, d, \beta)$. The probability P is calculated to show how it varies with the link length.

$$P(r,\alpha,d) = \int_\beta f(\beta)P(r,\alpha,d,\beta)d_\beta \tag{5.4}$$

where $f(\beta)$ is the probability density function of β for specific r, α and d. The receiver is uniformly distributed on the circle with d as the radius and the transmitter as the origin, or on part of the circle within the WPAN area if $R-r<d<R+r$ i.e., two circles in Fig. 5.1 intersect each other. Therefore, the pdf of β is

$$f(\beta) = \begin{cases} \dfrac{1}{2\pi}, & (0 \leq \beta < 2\pi,\ 0 < d \leq R-r) \\ \dfrac{1}{\beta_2 - \beta_1}, & (\beta_1 \leq \beta \leq \beta_2,\ R-r < d < R+r) \\ 0, & (R+r \leq d) \end{cases} \tag{5.5}$$

where β_1 is determined by

$$\cos\beta_1 = \frac{(R^2 - r^2 - d^2)\cos\alpha - \sin\alpha\sqrt{4R^2r^2 - (R^2 + r^2 - d^2)^2}}{2rd} \tag{5.6}$$

and

$$\sin\beta_1 = \frac{(R^2 - r^2 - d^2)\sin\alpha + \cos\alpha\sqrt{4R^2r^2 - (R^2 + r^2 - d^2)^2}}{2rd} \tag{5.7}$$

while

$$\cos\beta_2 = \frac{(R^2 - r^2 - d^2)\cos\alpha + \sin\alpha\sqrt{4R^2r^2 - (R^2 + r^2 - d^2)^2}}{2rd} \tag{5.8}$$

and

$$\sin\beta_2 = \frac{(R^2 - r^2 - d^2)\sin\alpha - \cos\alpha\sqrt{4R^2r^2 - (R^2 + r^2 - d^2)^2}}{2rd} \tag{5.9}$$

determine the value of β_2. Finally, the average probability that a transmitter lies outside of the beamwidth of the receiver and does not direct its beamwidth to the receiver is given by

$$\begin{aligned} P(d) &= \int_0^R \int_0^{2\pi} f(r,\alpha)P(r,\alpha,d)d_\alpha d_r & (5.10) \\ &= 4\int_0^R \int_0^{\frac{\pi}{2}} f(r,\alpha)P(r,\alpha,d)d_\alpha d_r & (5.11) \end{aligned}$$

where $f(r,\alpha)$ is the joint pdf of r and α. The transmitter is normally distributed in the WPAN area. Then the joint probability density function of r and α is

$$f(r,\alpha) = \frac{r}{\pi R^2} \quad (0 \leq \alpha < 2\pi,\ 0 < r \leq R) \tag{5.12}$$

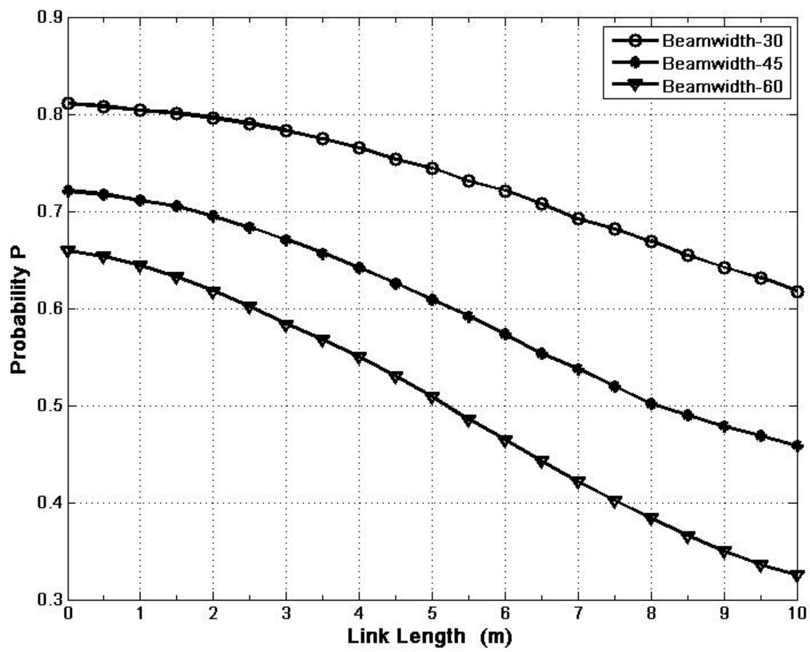

Figure 5.2: Probability P versus Link Length

Therefore, we can obtain the average probability that two links can transmit concurrently $Q = P^2(d)$, which indicates how the spatial multiplexing capacity varies with link distance on average. Fig. 5.2 shows the numerical results of probability P as a function of link length d with different antenna beamwidths. The probability P decreases as link length increases. Therefore, the proposed multi-hop concurrent transmission scheme, which replaces single long hop with multiple short hops, can explore more spatial reuse, i.e., it can allow more concurrent links with the same spatial resource. Fig. 5.2 also shows that the decrease trend of probability P slows down for small antenna beamwidth. An extreme case is that the concurrent transmission probability is a constant when antenna beamwidth is 0 degree.

5.2 Time Division Multiplexing

According to equation (3.4), link capacity varies with link length. Thus each link needs various number of time slots to transmit data if the required data rates are homogenous. The time slots allocated to each link in the concurrent transmission scheme are larger than or equal to the required number of slots because in the multi-hop concurrent transmission scheme, the assigned slots for a link are the maximum required time slots of all the links within the group. In Fig. 5.3 (a), a schedule is shown for SHCT scheme. The required time slots of link 2, 4, 5 and 8 are far less than the number of time slots reserved for the groups they are scheduled in. It can be expected to utilize the resource more efficiently by properly breaking the single long hop into multiple short hops. For example, as shown in Fig. 5.3 (b), by breaking the long hops (i.e., hop 1, 3, 6 and 7) into two short hops, the total number of slots for eight flows are reduced from 38 to 29 although the number of groups goes from 2 to 3, thus the flow throughput and network throughput are enhanced greatly. Replacing single long hop with multiple short hops can be likely to support more flows in a superframe. In the following, we theoretically show the time division multiplexing gain of multi-hop concurrent transmission (MHCT) scheme.

To make the performance of single hop and multi-hop concurrent transmission schemes comparable with time division multiplexing, the spatial multiplexing gain is fixed, i.e., the average number of concurrent links for each group in MHCT scheme is the same as that in SHCT scheme. The average number of concurrent links in each group is a function of concurrent transmission probability and the number of transmission links in the network. We assume that the concurrent transmission probability is a constant Q. The proposed hop selection metric prefers the relay nodes close to the line from source to destination, which constrains the concurrent transmissions for intra-flow hops. The half-duplex transmission and limited number of hops for each flow also enhance this constraint. Therefore it is assumed that the intra-flow hops do not transmit concurrently in the same

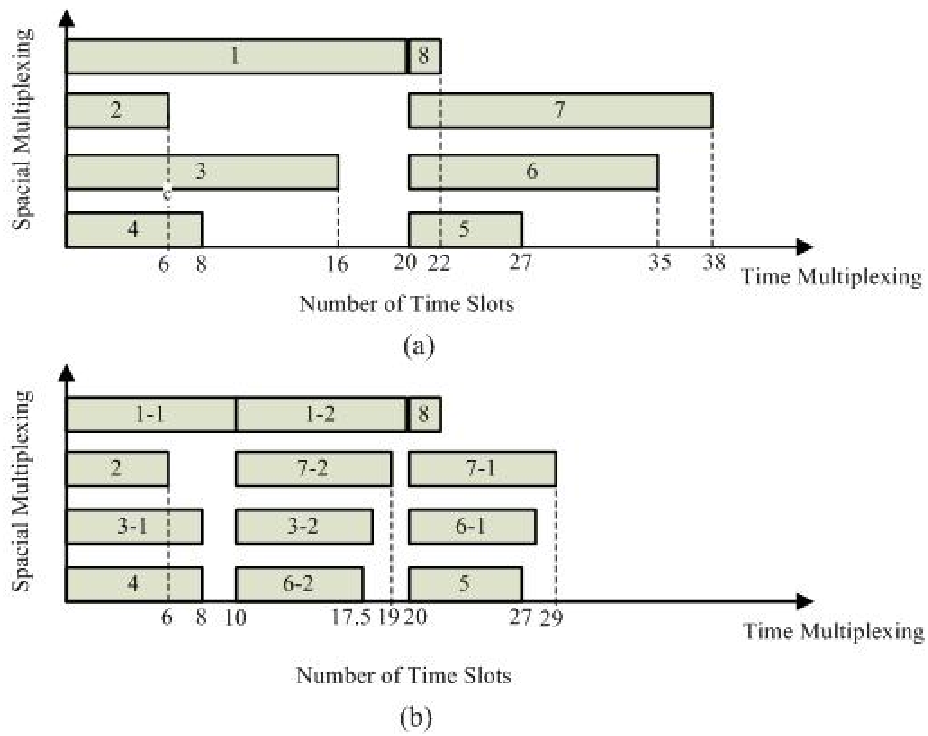

Figure 5.3: Illustration for Time Division Multiplexing

group. Consider N active flows in a WPAN, which means N independent hops in SHCT scheme and N' ($N' > N$) hops in MHCT scheme. Without concurrent transmissions for intra-flow hops, there are still N independent hops to be scheduled for each group in MHCT scheme. Therefore, the average number of concurrent hops for each group is almost the same for SHCT and MHCT schemes. $P(k, N)$ denotes the probability that only k hops satisfy concurrent transmission condition and can be scheduled in the same group among N hops. The probability that a hop does not conflict with any of the other $k-1$ hops is Q^{k-1}. Therefore,

$$P(k, N) = P(k-1, N-1)Q^{k-1} + P(k, N-1)(1-Q^k) \quad (5.13)$$

for $k = 1, 2, 3, \ldots, N$. We can iteratively obtain $P(k, N)$ by giving the initial condition $P(1, 1) = 1$, $P(1, 2) = 1 - Q$ and $P(2, 2) = Q$. If among N flows, the first flow can not transmit concurrently with the other N-1 flows,

$$P(1, N) = (1 - Q)^{N-1} \tag{5.14}$$

Another extreme case is that the N flows can be scheduled concurrently, which means that none of the flows conflict with others,

$$P(N, N) = (Q^{\frac{N-1}{2}})^N \tag{5.15}$$

The average number of concurrent transmissions in each group is

$$M = \sum_{k=1}^{N} kP(k, N) \tag{5.16}$$

The average number of groups for N single-hop flows is given by

$$G_N = \frac{N}{M} \tag{5.17}$$

while the average number of groups for N multi-hop flows can be obtained by

$$G_{N'} = \frac{N'}{M} \tag{5.18}$$

The average number of concurrent hops of each group for MHCT and SHCT schemes is the same without consideration of intra-flow concurrent transmissions.

The reserved slots for each group is defined as the maximum number of time slots among all the hops in this group, which is denoted by random variable X. The cdf of X is

$$F_X(x) = P(X \leq x) \tag{5.19}$$

and $P(X \leq x)$ can be obtained by

$$P(X \leq x) = P(X_1 \leq x, X_2 \leq x \dots X_M \leq x) \tag{5.20}$$

where X_m $(m = 1, 2, \dots, M)$ are the required number of time slots for each link in the group. Because the source and destination of each flow are randomly selected, X_m

$(m = 1, 2, \ldots, M)$ are i.i.d random variables with pdf $\widetilde{f}(x)$ for SHCT scheme. $X_m(m = 1, 2, \ldots, M)$ are also i.i.d with pdf $\overline{f}(x)$ for MHCT scheme without consideration of intra-flow concurrent transmissions. Therefore, we have

$$F_X(x) = P(X_1 \le x, X_2 \le x \ldots X_M \le x) \tag{5.21}$$

$$= \prod_{m=1}^{M} P(X_m \le x) \tag{5.22}$$

For SHCT scheme, given the pdf of $X_m(m = 1, 2 \ldots n)$, then

$$P(X_m \le x) = \int_0^x \widetilde{f}(x)dx \tag{5.23}$$

Substitute equation (5.23) into equation (5.22),

$$F_X(x) = [\int_0^x \widetilde{f}(x)dx]^M \tag{5.24}$$

The pdf of X can be given by

$$f_X(x) = \frac{dF_X(x)}{dx} = M\widetilde{f}(x)[\int_0^x \widetilde{f}(x)dx]^{M-1} \tag{5.25}$$

The expected number of time slots reserved for each group is

$$E[X] = \int_{x_a}^{x_b} x f_X(x)dx \tag{5.26}$$

$$= \int_{x_a}^{x_b} xM[\int_0^x \widetilde{f}(x)dx]^{M-1}\widetilde{f}(x)dx \tag{5.27}$$

$$= \int_{x_a}^{x_b} Mx[\widetilde{F}(x)]^{M-1}\widetilde{f}(x)dx \tag{5.28}$$

where x_a and x_b are the minimum and maximum required number of slots among all the hops in a group respectively. $\widetilde{F}(x)$ is the cdf of $X_m(m = 1, 2 \ldots M)$ in SHCT scheme and is defined as $\widetilde{F}(x) = \int_0^x \widetilde{f}(x)dx$. Then we have $\widetilde{F}(x_a) = 0$ and $\widetilde{F}(x_b) = 1$. The total required number of time slots for N single hop flows with SHCT scheme is

$$T_{SHCT} = \frac{N}{M}E[X] \tag{5.29}$$

$$= N\int_{x_a}^{x_b} x[\widetilde{F}(x)]^{M-1}\widetilde{f}(x)dx \tag{5.30}$$

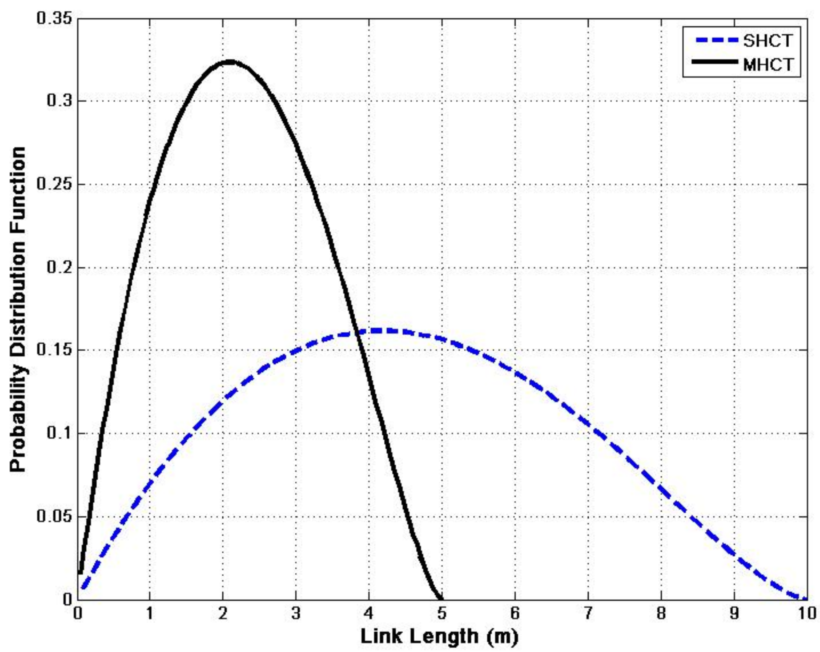

Figure 5.4: Probability Distribution Function of Link Length

Similarly, the total assigned time slots with MHCT scheme for N multi-hop flows is given by

$$T_{MHCT} = N' \int_{x'_a}^{x'_b} x[\overline{F}(x)]^{M-1}\overline{f}(x)dx \tag{5.31}$$

where $\widetilde{F}(x) = \int_0^x \widetilde{f}(x)dx$. To ensure that the MHTC scheme outperforms SHTC scheme in time division multiplexing, we should have $T_{MHCT} < T_{SHCT}$. Therefore, the condition that MHCT scheme can explore more time division multiplexing gain can be obtained:

$$\frac{N'}{N} < \frac{\int_{x_a}^{x_b} x[\widetilde{F}(x)]^{M-1}\widetilde{f}(x)dx}{\int_{x'_a}^{x'_b} x[\overline{F}(x)]^{M-1}\overline{f}(x)dx} \tag{5.32}$$

From equation (5.31), the total number of slots required for N flows with MHCT scheme depends on the total number of hops, the average number of concurrent hops and the distribution of required time slots for each hop. The total number of hops is determined by the number of hops used to replace the single long hop. The distribution of time slots relies on how to choose the relays for a multi-hop traffic flow. Therefore, the hop selection metric plays an crucial role on exploring the time division multiplexing gain in MHCT scheme. The ideal case is that all the N' hops are with the same length, which results in the fact that all the hops requires the same number of time slots. Then the optimal resource utilization efficiency is achieved. Our proposed hop selection metric works well on breaking the single long hop into short hops with homogeneous lengths. For hops with short link length, the link length square item in equation (4.1) makes small contributions to accumulated weights while it contributes greatly to accumulated weights for hops with long link length. Thus to get the minimum accumulated weights for a traffic flow, the proposed metric breaks a single long hop into more short hops than that for a single short hop. Therefore, the required numbers of time slots for hops in MHCT scheme are homogeneous. Without loss of generality, we choose $N' = 2N$ to show the numerical results. The probability distribution function of distance between two nodes randomly picked in a circle with radius R is found in [33]. The pdf of link length in MHCT scheme is obtained by shrinking the pdf of single hop link length by a half (see Fig. 5.4). The channel capacity is calculated according equation (3.4) with reference distance $d_{ref} = 1.5m$. Fig. 5.5 shows the required number of time slots for flows with MHCT scheme and SHCT scheme. We can see that the proposed multi-hop concurrent transmission scheme greatly improves the time division multiplexing gain. With MHCT scheme, it takes less time for the same number of flows to transmit data, thus the network throughout and flow throughput are increased.

5.3 Per-Flow Throughput

In this section, we analyze the per-flow throughput given a schedule. A schedule specifies for each slot, the set of links that are active in that slot. The flow throughput depends on the hops the flow goes over, and the concurrent transmission scheduling algorithm which

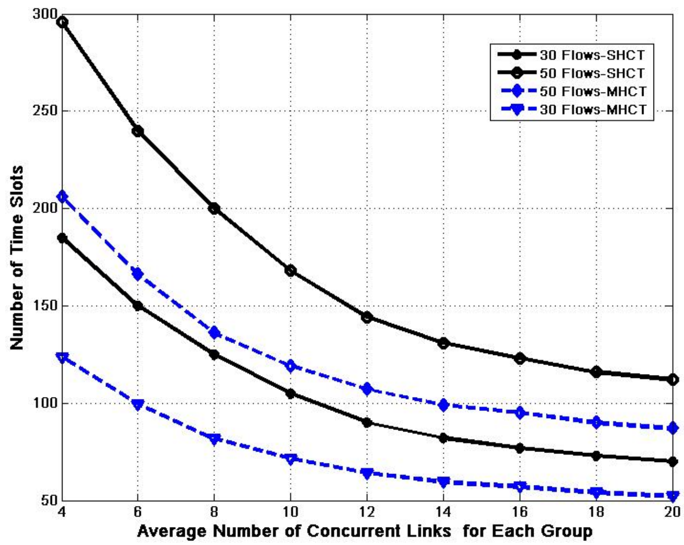

Figure 5.5: Time Division Multiplexing

assigns a number of slots to each flow. The flow throughput is defined as the ratio of the transmitted data for the flow to the time duration assigned to the flow. In the proposed concurrent transmission scheduling algorithm, a transmission request $r(i, j)$ for jth hop of ith flow requires $n(i, j)$ time slots. However, the time dedicated for hop j of flow i is larger than or equal to $n(i, j) \times \Delta t$ (Δt is the time duration of each slot)because we consider non-conflict hops as a group and allow them to transmit concurrently. The assigned slots for each group are the maximum required time slots of all the hops within the group. Let T_y denote the number of time slots reserved for yth group G_y in a valid schedule. If $r(i, j)$ is successfully scheduled in yth group

$$T(i, j) = T_y \tag{5.33}$$

where $T(i, j)$ is the time slots dedicated to jth hop of flow i in the schedule. The throughput of flow i is

$$F_i = \frac{C(i,j)n(i,j) \times \Delta T}{\sum_{y=1}^{Y} T_y I_{i,y}} \tag{5.34}$$

where $C(i,j)$ is the capacity of hop j of flow i. Since the nodes are static, and the links are line-of-sight, we assume that the link capacities are fixed. Y is the total number of groups in a valid schedule. $C(i,j)n(i,j) \times \Delta T$ is the data transmitted for flow i during the superframe. $\sum_{y=1}^{Y} T_y I_{i,y}$ is the time duration for flow i in each superframe. $I_{i,y}$ is the identification function:

$$I_{i,y} = \begin{cases} 1, & for\ any\ j,\ n(i,j) \in G_y \\ 0, & \text{otherwise} \end{cases} \tag{5.35}$$

Chapter 6

Performance Evaluation

In this chapter, we describe the evaluation methodology and present performance results for our proposed multi-hop concurrent transmission scheme compared with the traditional single hop transmission schemes.

We evaluate the performance of the proposed scheme in a typical indoor environment where 60 GHz WPAN is expected to be deployed, e.g., a large office space. As shown in Fig. 6.1, the PNC is placed in the center of the room with 16×16 square meters and a total of 40 WNs are randomly distributed in the room. Each node is equipped with a directional antenna with a beamwidth of 60 degrees, corresponding to six beams at each node. A node can communicate with all other nodes within its transmission range if the LOS link is available. The moving obstacles located within the LOS link cause severe data rate reduction in that link. Therefore, we assume that for each link, the obstacles located in LOS link is with probability p and the time interval for obstacles to stay in LOS link is T_{NLOS}. According to equation (3.4), the received power increases with a decrease in link length r. The maximum data rate is achieved at the reference distance d_{ref}. The corresponding path loss at d_{ref} is PL_0. The parameters used in our simulations are listed in Table 6.1. The simulations consist of different numbers of traffic flows in the mmWave

Parameters	**Symbol**	**Value**
System bandwidth	W	1200 MHz
Transmission power	P_T	0.1mW
Background noise	N_0	-134dBm/MHz
Path loss exponent	n	2
Reference distance	d_{ref}	1.5m
Path loss at d_{ref}	PL_0	71.5 dB
Slot time	Δt	$18\mu s$
Number of slots in transmission period	N	1000
Probability of NLOS link	p	0.1
NLOS period for each link	T_{NLOS}	0.2ms

Table 6.1: SIMULATION PARAMETERS

WPAN and each traffic flow is transmitted between a pair of randomly chosen nodes. The traffic flow at the source node is CBR flow with holding time uniformly distributed between 0.5 minute and 2 minutes.

We study the throughput of three transmission schemes: multi-hop concurrent transmission (MHCT), single hop concurrent transmission (SHCT) [23] and single hop transmission (SHT) to support P2P transmission in mmWave WPAN. In the single hop concurrent transmission scheme, if LOS link is unavailable, a neighboring WN is randomly chosen to relay the traffic. We use the single hop transmission scheme operating in a TDMA mode as a baseline for comparison.

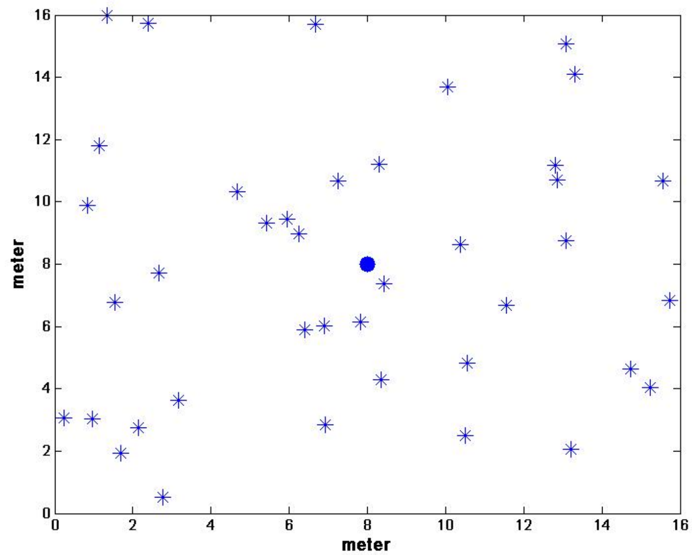

Figure 6.1: Node Placement for Simulation Scenario

6.1 Average Flow Throughput

Fig. 6.2 shows the average flow throughput versus various numbers of traffic flows in the network. It can be seen that the MHCT scheme provides much higher flow throughput on average, which is essential for mmWave WPAN to support bandwidth-intensive applications. In our scheme, multiple hops of a traffic flow can concurrently transmit if they do not conflict with each other. The average flow throughput decreases with the increase of the number of flows because more traffic flows compete for the limited network resources. From Fig. 6.2, we find that the proposed multi-hop concurrent transmission scheme outperforms both SHCT and SHT on average flow throughput. The main reason for average flow throughput improvement is the time division multiplexing gain resulting from multi-hop concurrent transmissions.

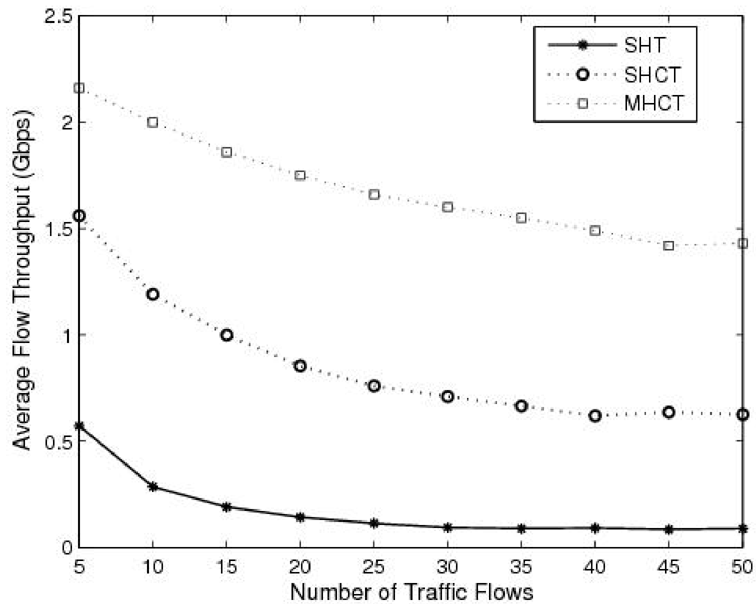

Figure 6.2: Average Flow Throughput versus Various Number of Traffic Flows

6.2 Network Throughput

The network throughput is shown in Fig. 6.3. The SHT scheme is a TDMA transmission scheme and there is at most one transmission in the network at any given time. So the network throughput does not vary much for various numbers of flows in the network. The concurrent transmission can significantly increase the network throughput. It is also shown that the proposed MHCT scheme achieves higher network throughput compared with SHCT scheme. The following are the main contributions to network throughput improvement in MHCT scheme: 1) By breaking a single long hop into several short hops, the transmission data rate for each hop becomes larger. 2) The proposed scheme can provide higher concurrent transmission probability and involve more hops in each group to transmit concurrently. 3) The MHCT scheme obtains more efficient time resource utilization.

In summary, the proposed multi-hop concurrent transmission scheme, considering the

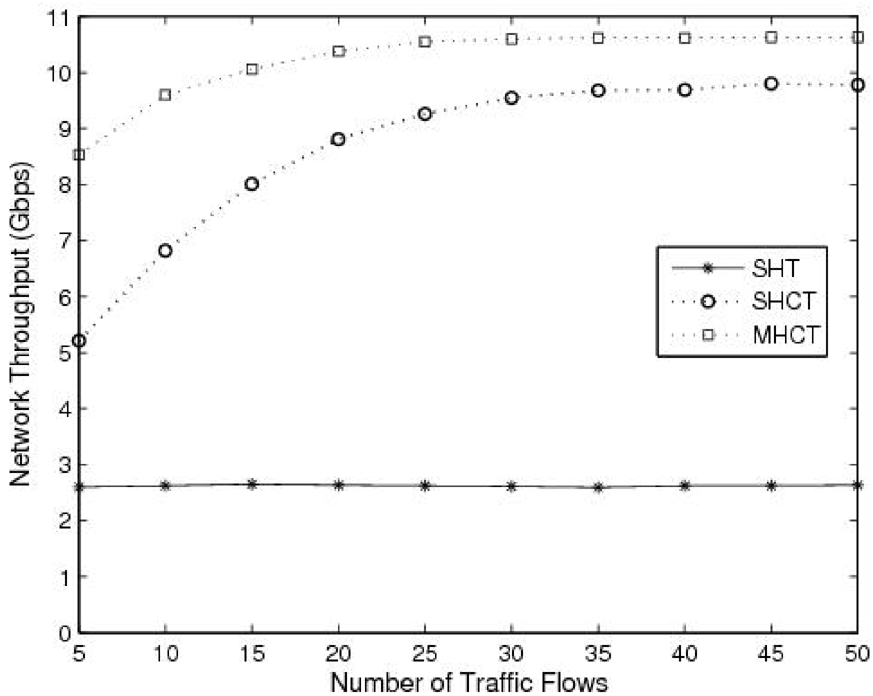

Figure 6.3: Network Throughput versus Various Number of Traffic Flows

unique characteristics of mmWave WPAN, improves the network performance significantly on network throughput and flow throughput by exploiting more time multiplexing gain and spatial multiplexing gain.

Chapter 7

Conclusions

mmWave WPAN is promising to provide high data rate (Gbps) for bandwidth-intensive indoor applications. Existing transmission schemes of WPAN do not take into account the unique characteristics of mmWave band. It is necessary to design a novel transmission scheme for mmWave WPAN to improve the resource utilization and realize Gbps transmission.

In this thesis, a multi-hop concurrent transmission scheme is proposed for mmWave WPAN. Taking the unique characteristics of mmWave WPAN (i.e., high propagation loss, LOS link and directional antenna) into consideration, the proposed MHCT scheme achieves great improvement on spatial reuse and time division multiplexing, thus significantly increases network throughput and traffic flow throughput. By replacing a single long hop with multiple short hops using the MHCT scheme, the concurrent transmission probability becomes larger than that based on traditional SHCT scheme in WPAN. The MHCT scheme, which deploys time division multiplexing, outperforms the SHCT scheme. In addition, we analyze the performance of the proposed scheme in terms of per-flow throughput. The simulation results demonstrate that the proposed scheme significantly improves the traffic flow throughput, network throughput and resource utilization efficiency. The mmWave

WPAN with our proposed multi-hop concurrent transmission scheme can provide higher data rate to enable the numerous multimedia applications requiring large bandwidth. The results should provide important guidelines for future research of mmWave WPAN, such as enabling multi-hop transmissions and improving the resource utilization efficiency on spatial reuse and time division multiplexing.

7.1 Future works

By properly breaking a single long hop into multiple short hops, the proposed MHCT scheme can exploit more spatial reuse gain and utilize time resource more efficiently in comparison to SHCT scheme and TDMA mode transmission. To further improve the resource utilization efficiency, there is another significant issue to be addressed. There are many transmission requests in the queue waiting to be scheduled. Which is to be scheduled first? Different scheduling sequences give different schedules, which specifies the set of links that are active in each time slot in a superframe. In other words, with the same transmission requests, we can obtain various combinations of groups in the scheduling scheme without consideration on scheduling sequence of the transmission requests. There must be one combination of the concurrent groups (i.e., a specific schedule), which requires minimum number of time slots for transmission requests to be scheduled.

In the REX scheme in [23] and our proposed scheme, the PNC sequentially checks the transmission requests and allows non-conflicting communication links to be scheduled concurrently based on concurrent transmission condition. In [26], the VTSA scheme does not specify the scheduling sequence for numerous communication links although it allows multiple communication links to transmit concurrently. In [34], a joint routing and scheduling scheme is proposed to satisfy maximum fraction of each traffic flow demand, but it takes much communication overheads and computing overheads, especially for implementing it to mmWave WPAN because of the limited power of PNC. In our future work, an optimization model will be developed to formulate the above problem, aiming to obtain the minimum number of time slots for a number of transmission requests to be scheduled. This problem is NP-hard. Based on the model, a sub-optimal algorithm would be proposed to divide the transmission requests into several groups in order to achieve higher flow throughput and network throughput with acceptable computation of overheads.

Another critical issue to be addressed in mmWave WPAN is power control due to the high carrier frequency (i.e., 60 GHz band). A typical approach for energy saving is to shift the node into the sleep mode when it has no data to send. The sleeping node wakes up periodically to receive the data from other nodes. Other approaches use a power control scheme during transmission. In the case of using MIMO, which is highly likely in millimeter-wave systems, a transceiver can further save the power by switching other antenna chains off and leaving only one working antenna chain to monitor the network. The power saving mode needs the support of the MAC protocol. The dilemma of power control is the following: power control can reduce the interferences and can allow more communication links to transmit data simultaneously, which improves the spatial reuse. However, to achieve higher data rate, the transmitter needs to use more power, which increases the interference resulting in throughput reduction [35].

Power control is also helpful in alleviating the hidden terminal problem. The transmission power can be effectively controlled so as to control the transmission range of a node. With channel knowledge from neighbor nodes, a hidden node can adjust its transmitting power in a way that the ongoing transmission will not be disrupted. A joint optimization process to maximize the battery life, make the network stable, and improve the system performance and capacity is a highly challenging task.

In order to give a comprehensive evaluation of the proposed multi-hop concurrent transmission scheme and make it more practical, transmission failure scenarios should be considered with the corresponding recover mechanisms. Several scenarios are listed as follows.

1. Transmission request is blocked by the moving obstacles.
2. Transmission request arrives at PNC, but PNC does not receive it due to the transmission collision in random access period.
3. PNC receives the transmission request, but the scheduling information can not be delivered to wireless node due to the moving obstacles.
4. One hop is blocked while other hops in the same traffic flow transmit data successfully.

Bibliography

[1] T. Manabe, Y. Miura, and T. Ihara, "Effects of Antenna Directivity and Polarization on Indoor Multipath Propagation Characteristics at 60 GHz," *IEEE J. Sel. Areas Commun.*, vol. 14, no. 3, pp. 441–448, 1996.

[2] P. Smulders, "Exploiting the 60 GHz Band for Local Wireless Multimedia Access: Prospects and Future Directions," *IEEE Commun. Mag.*, vol. 40, no. 1, pp. 140–147, Jan. 2002.

[3] P. Smulders, H. Yang, and I. Akkermans, "On the Design of Low-Cost 60-GHz Radios for Multigigabit-per-Second Transmission over Short Distances [Topics in Radio Communications]," *IEEE Commun. Mag.*, vol. 45, no. 12, pp. 44–51, Dec. 2007.

[4] C. Park and T. Rappaport, "Short-Range Wireless Communications for Next-Generation Networks: UWB, 60 GHz Millimeter-Wave WPAN, and ZigBee," *IEEE Wireless Commun.*, vol. 14, no. 4, pp. 70–78, Aug. 2007.

[5] R. Daniels and R. Heath, "60 GHz Wireless Communications: Emerging Requirements and Design Recommendations," *IEEE Veh. Technol. Mag.*, vol. 2, no. 3, pp. 41–50, Sept. 2007.

[6] J. Foerster, J. Lansford, J. Laskar, T. Rappaport, and S. Kato, “Realizing Gbps Wireless Personal Area Networks,” *IEEE J. Sel. Areas Commun.*, vol. 27, no. 8, pp. 1313–1317, Oct. 2009.

[7] C. Anderson and T. Rappaport, “In-building Wideband Partition Loss Measurements at 2.5 and 60 GHz,” *IEEE Trans. Wireless Commun.*, vol. 3, no. 3, pp. 922–928, May 2004.

[8] H. Xu, V. Kukshya, and T. S. Rappaport, “Spatial and Temporal Characteristics of 60-GHz Indoor Channels,” *IEEE J. Select. Areas Commun.*, vol. 20, no. 3, pp. 620–630, April 2002.

[9] “IEEE 802.15 WPAN Millimeter Wave Alternative PHY Task Group 3c(TG3c),” http://www.ieee802.org/15/pub/TG3c.html, 2010.

[10] “IEEE 802.11 VHT Study Group,” http://www.ieee802.org/11/Reports/vht_update.htm, 2010.

[11] “ECMA International TC48 High Rate Short Range Wireless Communications,” http://www.ecma-international.org/memento/TC48-M.htm, 2010.

[12] S. Singh, F. Ziliotto, U. Madhow, E. Belding, and M.J.W.Rodwell, “Millimeter Wave WPAN: Cross-Layer Modeling and Multihop Architecture,” in *Proc. IEEE INFOCOM*, May 2007, pp. 2336–2240.

[13] S. Emami, C. Doan, A. Niknejad, and R. Brodersen, “A Highly Integrated 60GHz CMOS Front-End Receiver,” in *Proc. IEEE International Solid-State Circuits Conference*, Feb. 2007, pp. 190–192.

[14] C. Doan, S. Emami, A. Niknejad, and R. Brodersen, “Millimeter-wave CMOS Design,” *IEEE J. Solid-State Circuits*, vol. 40, no. 1, pp. 144–155, Jan. 2005.

[15] C. H. Wang, Y. H. Cho, C. S. Lin, H. Wang, C. H. Chen, D. C. Niu, J. Yeh, C. Y. Lee, and J. Chen, "A 60GHz Transmitter with Integrated Antenna in 0.18um SiGe BiCMOS Technology," June 2006, pp. 659–668.

[16] H. Singh and S. Singh, "Smart-aloha for Multi-hop Wireless Networks," *Mob. Netw. Appl.*, vol. 10, no. 5, pp. 651–662, 2005.

[17] G. Jakllari, W. Luo, and S. V. Krishnamurthy, "An Integrated Neighbor Discovery and MAC Protocol for Ad Hoc Networks Using Directional Antennas," in *Proc. IEEE WOWMOM*, 2005, pp. 11–21.

[18] T. Korakis, G. Jakllari, and L. Tassiulas, "CDR-MAC: A Protocol for Full Exploitation of Directional Antennas in Ad Hoc Wireless Networks," *IEEE Trans. Mob. Comput.*, vol. 7, no. 2, pp. 145–155, Feb. 2008.

[19] N. Guo, R. C. Qiu, S. S. Mo, and K. Takahashi, "60-GHz Millimeter-Wave Radio: Principle, Technology, and New Results," *EURASIP J. Wirel. Commun. Netw.*, vol. 7, no. 1, pp. 48–58, Feb. 2007.

[20] R. Ramanathan, J. Redi, C. Santivanez, D. Wiggins, and S. Polit, "Ad Hoc Networking with Directional Antennas: A Complete System Solution," *IEEE J. Select. Areas Commun.*, vol. 23, no. 3, pp. 496–506, March 2005.

[21] L. X. Cai, X. Shen, and J. W. Mark, "Efficient MAC Protocol for Ultra-wideband Networks," *IEEE Communications Magazine*, vol. 47, no. 6, pp. 179–185, June 2006.

[22] S. Singh, F. Ziliotto, U. Madhow, E. Belding, and M. Rodwell, "Blockage and Directivity in 60GHz Wireless Personal Area Networks: From Cross-Layer Model to Multihop MAC Design," *IEEE J. Sel. Areas Commun.*, vol. 27, no. 8, pp. 1400–1413, Oct. 2009.

[23] L. X. Cai, L. Cai, X. Shen, and J. Mark, "REX: A Randomized EXclusive Region Based Scheduling Scheme for mmWave WPANs with Directional Antenna," *IEEE Trans. on Wireless Commun.*, vol. 9, no. 1, pp. 113–121, Jan. 2010.

[24] L. X. Cai, L. Cai, X. Shen, and J. W. Mark, "Spatial Multiplexing Capacity Analysis of mmWave WPANs with Directional Antennae," in *Proc.IEEE GLOBECOM*, Nov. 2007, pp. 4744–4748.

[25] J. Wang, R. Prasad, and I. Niemegeers, "Enabling Multi-hop on mmWave WPANs," in *Proc. IEEE ISWCS*, Oct. 2008, pp. 371–375.

[26] C. Sum, Z. Lan, R. Funada, J. Wang, T. Baykas, M. Rahman, and H. Harada, "Virtual Time-Slot Allocation Scheme for Throughput Enhancement in a Millimeter-Wave Multi-Gbps WPAN System," *IEEE J. Sel. Areas Commun.*, vol. 27, no. 8, pp. 1379–1389, Oct. 2009.

[27] J. Wang, Z. Lan, C. W. Pyo, T. Baykas, C. Sum, M. Rahman, J. Gao, R. Funada, F. Kojima, H. Harada, and S. Kato, "Beam Codebook Based Beamforming Protocol for Multi-Gbps Millimeter-Wave WPAN Systems," *IEEE J. Sel. Areas Commun.*, vol. 27, no. 8, pp. 1390–1399, Oct. 2009.

[28] C. W. Pyo and H. Harada, "Throughput Analysis and Improvements of Hybrid Multiple Access in IEEE 802.15.3c mmWave-WPAN," *IEEE J. Sel. Areas Commun.*, vol. 27, no. 8, pp. 1414–1424, Oct. 2009.

[29] M. Park and P. Gopalakrishnan, "Analysis on Spatial Reuse and Interference in 60-GHz Wireless Networks," *IEEE J. Sel. Areas Commun.*, vol. 27, no. 8, pp. 1443–1452, Oct. 2009.

[30] S. Y. Geng, J. Kivinen, X. W. Zhao, and P. Vainikainen, "Millimeter-Wave Propagation Channel Characterization for Short-Range Wireless Communications," *IEEE Trans. Veh. Technol.*, vol. 58, no. 1, pp. 3–13, Jan. 2009.

[31] R. Mudumbai, S. Singh, and U. Madhow, "Medium Access Control for 60 GHz Outdoor Mesh Networks with Highly Directional Links," in *Proc. IEEE INFOCOM*, April 2009, pp. 2871–2875.

[32] L. X. Cai, L. Cai, X. Shen, and J. W. Mark, "Resource Management and QoS Provisioning for IPTV over mmWave-based WPANs with Directional Antenna," *ACM Mobile Networks and Applications(MONET)*, vol. 14, no. 2, pp. 210–219, Apirl 2009.

[33] http://mathworld.wolfram.com/DiskLinePicking.html, 2010.

[34] P. Dutta, V. Mhatre, D. Panigrahi, and R. Rastogi, "Joint Routing and Scheduling in Multi-hop Wireless Networks with Directional Antennas," in *Proc. IEEE INFOCOM*, March 2010, pp. 1–5.

[35] B. Radunovic and J. L. Boudec, "Optimal Power Control, Scheduling, and Routing in UWB Networks," *IEEE J. Sel. Areas Commun.*, vol. 22, no. 7, pp. 1252–1270, Sep. 2004.

[36] "Multi-Gb/s 60GHz Wireless Transceiver Design for Mobile Applications at Berkeley Wireless Reaearch Center," http://bwrc.eecs.berkeley.edu/Research/e-eis/60ghz_trans.html, 2009.

[37] "IBMs 60-GHz Page," http://www.ieee802.org/15/pub/TG3c.html, 2009.

[38] F. Gutierrez, S. Agarwal, K. Parrish, and T. Rappaport, "On-Chip Integrated Antenna Structures in CMOS for 60 GHz WPAN Systems," *IEEE J. Sel. Areas Commun.*, vol. 27, no. 8, pp. 1367–1378, Oct. 2009.

[39] H. Jiang, K. H. Liu, W. Zhuang, and X. Shen, "An Effective Resource Management Scheme for UWB Networks with Simultaneous Transmissions," *IEEE Trans. Wireless Commun.*, vol. 6, no. 8, pp. 3005–3015, Aug. 2007.

[40] K. H. Liu, L. Cai, and X. Shen, "Multi-class Utility-based Scheduling for UWB Networks," *IEEE Trans. Veh. Technol.*, vol. 57, no. 2, pp. 1176–1187, March 2008.

[41] A. Rangnekar and K. M. Sivalingam, "QoS Aware Multi-channel Scheduling for IEEE 802.15.3 Networks," *Mob. Netw. Appl.*, vol. 11, no. 1, pp. 47–62, Feb. 2006.